Journal of Information Engineering and Applications
ISSN 2224-5782 (print) ISSN 2225-0506 (online)
Vol 2, No.10, 2012

Radar Waveform Generation and Optimization based on Rossler Chaotic System

Joseph Obadha[1*] Stephen Musyoki[2] George Nyakoe[3]

1. Department of Telecommunication and Information Engineering, Jomo Kenyatta University of Agriculture and Technology, P. O. Box 6200-00200, Nairobi, Kenya
2. Department of Telecommunication and Information Engineering, Jomo Kenyatta University of Agriculture and Technology, P. O. Box 6200-00200, Nairobi, Kenya
3. Department of Mechatronics, Jomo Kenyatta University of Agriculture and Technology, P. O. Box 6200-00200, Nairobi, Kenya

* E-mail of the corresponding author: josephabok@yahoo.co.uk

Abstract

The concept of Multiple-Input Multiple-Output (MIMO) radars has drawn considerable attention recently. Unlike the traditional Single-Input Multiple-Output (SIMO) radar which emits coherent waveforms to form a focused beam, the MIMO radar can transmit orthogonal (incoherent) waveforms. These waveforms can be used to increase the system spatial resolution. The challenge is on how to generate the large set of incoherent waveforms. Contemporary research has focused on using chaotic systems to generate these waveforms. With Chaotic waveforms obtained from a dynamical system, different radar waveforms can be generated from a single dynamical system; one only needs to change the control parameters and the initial conditions of the system. This scheme for radar waveform generation reduces the need for a comprehensive library of waveforms in a radar system and generates waveforms with good properties for both secure communications and high spatial resolution.

This paper proposes the use of Rossler system– a type of a dynamical system to generate radar waveforms. Through Matlab/Simulink Simulations, it is shown that the Rossler waveforms, which are characterized by control variables and initial conditions are comparable to the Linear Frequency Modulated (LFM) waveforms, the most commonly used class of radar waveforms in terms of the ambiguity diagram and the frequency components and yet versatile enough to generate a large number of independent waveforms. An ambiguity diagram is a plot of an ambiguity function of a transmitted waveform and is a metric that characterizes the compromise between range and Doppler resolutions. It is a major tool for analyzing and studying radar waveforms. Impulsive synchronization theory is used to develop the ambiguity diagram.

Keywords: Chaos, Rossler system, ambiguity function, impulsive synchronization theory

1. Introduction

Radar (Radio detection and ranging) is an electromagnetic system for the detection and location of objects. A portion of the transmitted signal is intercepted by a reflecting object (target) and is reradiated in all directions. The antenna collects the returned energy in the backscatter direction and delivers it to the receiver. The distance to the receiver is determined by measuring the time taken for the electromagnetic signal to travel to the target and back. If there is a relative motion between the radar and the target there is a shift in frequency of the reflected signal (Doppler effect) which is a measure of the radial component of the relative velocity.

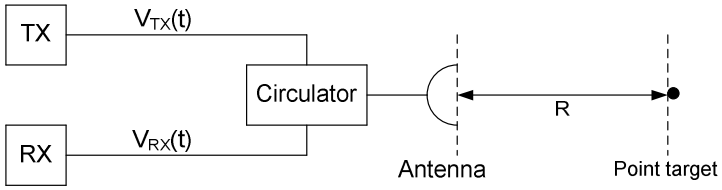

Figure 1: Simple Radar Model

The specifications of the waveform employed by any radar system have always been a key factor in determining performance and application. Radar systems typically utilize wideband waveforms that possess a narrow auto correlation main lobe, called the ambiguity function, in order to achieve fine range resolution. Waveform design problem based on optimization of the ambiguity function has been well studied (Levanon, N. and Mozeson, E., 2004). For a given specification of the radar waveform, the resulting quantification of range and Doppler resolution is elegantly captured in the ambiguity diagram derived from the ambiguity function as first postulated by Woodward (1967). The wideband radar waveform of choice is usually the Linear Frequency Modulation (LFM) waveform. It is wide spread use is mostly due to specific properties that allow for stretch processing, as explained in Skolnic (2001). However linear FM waveform has some disadvantages. For example they have high range side lobes, unless spectral tapering is applied to the receive signal (which sacrifices range resolution and degrades the signal to noise ratio). Furthermore the set of linear-FM waveforms includes only two quasi orthogonal waveforms, that is, the 'up-chirp,' and 'down chirp'. Many emerging radar applications often require a set of hundreds or even thousands of distinct quasi-orthogonal waveforms. In a quasi orthogonal waveform set, no single waveform significantly interferes with the detection of another waveform that is transmitted in the same frequency band and/or at the same time. An example of a radar system that requires a quasi orthogonal set is a multiple-input, Multiple-Output (MIMO) radar system. A MIMO radar system consists of multiple apertures, where each aperture is capable of transmitting and receiving radar waveforms.

Despite the use of pulse compression and other modulation techniques to achieve high range resolution, reliable classification of a broad range of targets in a wide variety of conditions still remains elusive. In recent years, with their noise-like property in the time domain and broadband characteristics in the frequency domain, possibilities of exploiting chaotic signals radar have been studied by many researchers. The first work incorporating the concept of chaos in radar involved the investigation of the ambiguity function of a chaotic phase modulated waveform (Lin, F. Y. and Liu J. M., 2004). Performance of chaotic frequency modulation (FM), amplitude modulation (AM), Phase modulation (PM) and pulse modulation radars have been reported (Carrol, T. L. and Pecora, L. M., 1991). In most of these works chaotic signals were generated by discrete map and employed in a radar system as baseband signal for modulation such as PM, FM and as a result this limits the bandwidth of the transmitted signal which in turn does not meet the requirements for ultra wideband radar signal. The random transmitted signal in addition to having the merit of high range resolution (Das, A. and Lewis, F. L., 2010), also has very low probability of intercept. One of the chaotic systems which have been extensively studied for the possibility of generating the chaotic radar signals is the Lorenz system (Willsey, M., 2006).

The contribution of this paper is to use a specific chaotic system, the Rossler system for waveform generation by appropriately selecting the system parameters. Specifically section 2 outlines the salient characteristics of the Rossler system and how the control parameters affect its behavior, Section 3 the mathematical formulation and methodology, section 4 Simulation results and discussion while Section 5 concludes the paper.

2. Theory

In 1976, Otto E Rossler (Rossler, O. E., 1976a) constructed the following three-dimensional system of differential equations

$$\frac{dx}{dt} = -y - z \tag{1}$$

$$\frac{dy}{dt} = x + ay \tag{2}$$

$$\frac{dz}{dt} = b + z(x - c) \tag{3}$$

where a, b and c are the static or control parameters and x, y and z are dynamic parameters. The original Rossler chaotic system had the parameters of $a = b = 0.2$ and $c = 5.7$. Changing the control parameters changes the behavior of the system and the system is said to undergo bifurcations. Figure 2 shows that as c is decreased periodic doubling occur at $b \cong 1.4$. Periodic doubling further occurs at $b \cong 0.6$. Towards $b \cong 0.2$ the curves seem to expand explosively and merge together to produce an area of almost solid blue. This behavior is an indicative of the onset of chaos and the value $b \leq 0.2$ can be used instead of $b = 0.2$ which has traditionally been used in this system to realize the chaos operating mode.

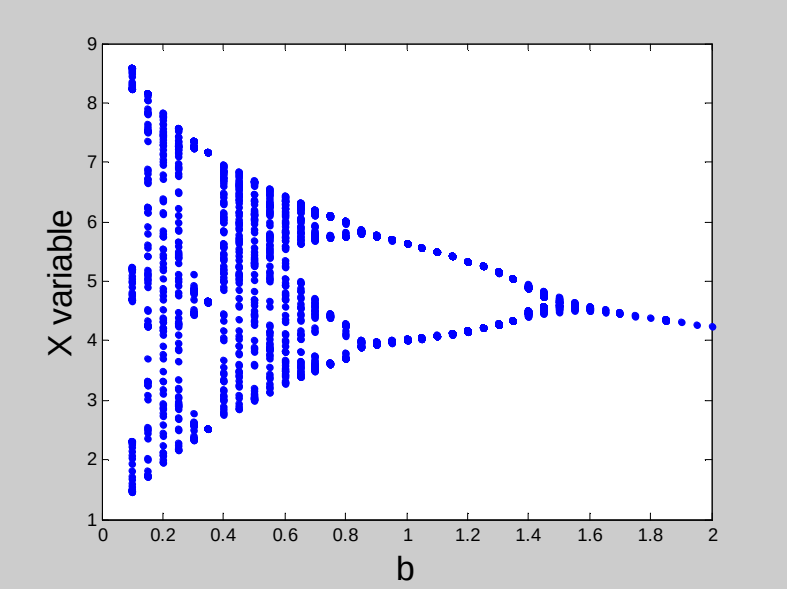

Figure 2: Onset of Chaos with b as the bifurcation parameter

A time series of x, y and z is shown in Figure 3. The initial conditions can be chosen arbitrarily. From direct observation of the time series, it is reasonable to say the x, y and z variables are aperiodic.

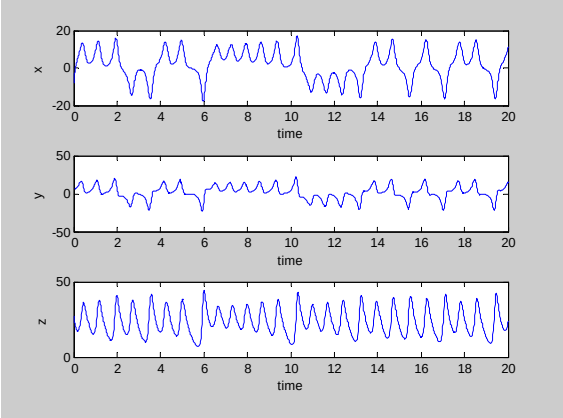

Figure 3: Time series of x, y and z variables

Chaotic systems exhibit sensitivity to initial conditions. For a chaotic system, two solutions with nearby initial conditions exponentially diverge. To demonstrate that the Rossler system has this sensitivity, the x state variable from two distinct solutions with nearby initial conditions are shown in Figure 4. In this Figure the graph labelled x_1 is obtained with the initial conditions of $x = [-8, 8, 27]$ while that labeled x_2 is obtained with the initial condition $x = [-7.8, 7.8, 26.8]$. As can be seen the two signals begin nearby and rapidly diverge from each other. Although only $x(t)$ is shown, the same behavior can be observed for both $y(t)$ and $z(t)$.

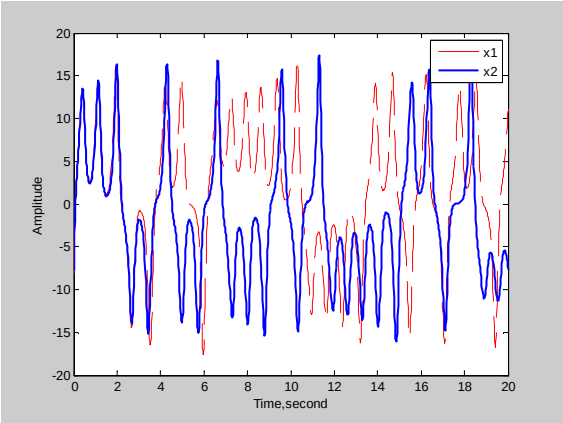

Figure 4: State variable x: Different initial conditions

Because of their quasi unpredictable behavior these signals are very appropriate for use in communication because of inherent security mechanism and spectral diversity.

3. Mathematical formulation

3.1 Frequency Spectrum of the Rossler Waveform

Mathematically time scaling the Rossler equations can be used to control the bandwidth of the state variables. Also scaling the parameters can be used to time and amplitude scale the state variables. The variable $\underline{x}(t)$ is defined as shown in Equation (4) where x, y and z denote the state variable of the Rossler system.

$$\underline{x}(t) = \begin{pmatrix} x(t) \\ y(t) \\ z(t) \end{pmatrix} \tag{4}$$

Next the $f\left(\underline{x}(t)\right)$ is defined as

$$f\left(\underline{x}(t)\right) = \begin{pmatrix} -y - z \\ x + ay \\ b + z(x - c) \end{pmatrix} \tag{5}$$

Therefore the Rossler system can be written as shown in Equation (6)

$$\dot{\underline{x}}(t) = f\left(x(t)\right) \tag{6}$$

For notational convenience $\underline{x}$ and $f(x)$ can be defined by dropping the t-dependence. Using this notation let $x(t)$ denote the solution to Equation (7). Also let $\tilde{\underline{x}}(t)$ denote the solution to Equation (8) where q is a constant greater than zero.

$$\dot{\underline{x}} = f(x) \tag{7}$$

$$\dot{\tilde{\underline{x}}} = qf(\tilde{x}) \tag{8}$$

If both systems have identical initial conditions then $\tilde{\underline{x}}(t)$ and $\underline{x}(t)$ are related as described in Equation (9)

$$\tilde{\underline{x}}(t) = \underline{x}(qt) \tag{9}$$

In other words scaling the Rossler equation by q (as shown in Equation (8) has the effect of time scaling $\underline{x}(t)$ by q. Scaling $\underline{x}(t)$ by q in time domain also scales the bandwidth of $\underline{x}(t)$ by q. The Fourier relationship in Equation (10) describes how this time scaling affects the bandwidth of $x(qt)$(Where $X(j\omega)$ is the Fourier transform of $x(t)$).

$$x(qt) \leftrightarrow \frac{1}{|q|} X\left(\frac{j\omega}{q}\right) \tag{10}$$

It will be shown through simulation that with the variation of the scaling factor p and the initial conditions x_0, y_0, z_0 the bandwidth of the Rossler waveform can be varied to a desired value.

3.2 Ambiguity function of the Rossler waveform (Impulsive Synchronization Theory)

The ambiguity function of a waveform can be evaluated from the general expression given in Equation 11 (Levanon, N. and Mozeson, E., 2004). It is used to measure the ability of a radar waveform to measure delay and Doppler shift. It represents the output of a matched filter for the waveform.

$$|\chi(\tau, f_d)|^2 = \left| \int_{-\infty}^{\infty} u(t)\, u^*(t+\tau) e^{j2\pi f_d t} dt \right|^2 \tag{11}$$

In the equation u(t) is the radar waveform under consideration and τ is the time delay. This two dimensional function indicates the matched filter output in the receiver when a delay mismatch τ and a Doppler mismatch f_d occur. The value $|\chi(0,0)|^2$ represents the matched filter output without mismatch. Therefore the higher the function $|\chi(0,0)|^2$ around (0,0) the better the Doppler and range resolution.

For the chaotic signals, the analytical treatment is not possible and in this section, impulsive synchronization scheme (Pecora, L. M. and Carrol, T. L., 1988; Lu, W. L., 2007; Lewis F. L. and Das, A. , 2011;Lu, J. G. , 2010; Cheng , Hu et al ,2010;Hu, H.P. and Zhu, Z. , 2010) is used to obtain the ambiguity diagram of the Rossler based signals for comparison with the LFM signal, the most commonly used radar signal. Consider two dynamical systems (Carrol, T. L. and Pecora, L. M., 1991)

$$\dot{x} = Ax + F(x) \tag{12}$$

$$\dot{y} = sAy + sF(y) \tag{13}$$

where F:$R^n \rightarrow R^n$ is continuous (F is a function that maps n dimensional vector space into an n dimensional vector space which is continuous), $x, y \in R^n$ (x, y are members of the n dimensional vector space, that is $x^T = [x_1, x_2, x_3]$ and $y^T = y_1, y_2, y_3$) are state variables, $A \in R^{n \times n}$ (A is a member of the $n \times n$ matrix) is a constant matrix, s is a constant and $\dot{x}$ and $\dot{y}$ indicate the dx/dt and dy/dt respectively. Suppose that the solution of equation (12) is $x(t)$ with initial conditions $x(0)$ then the system in Equation (13) has a solution of

$$y(t) = x(st) \tag{14}$$

when the initial condition $y(0)$ is set to be $x(0)$. Obviously y(t) is the time scaling version of $x(t)$ and can be obtained by solving Equation (13). It should be noted that equation (14) holds only when the two initial conditions are the same, because the systems work in chaotic states. Equation (14) also implies that the solution of Equation (13) is synchronized to the time-scaling solution of Equation (12). The scheme for generating time scaling chaotic signal is shown in Figure 5 which is outlined in the synchronization framework (Tao, Y. and Chuo, L.O., 1997). The driving system described by Equation (12) outputs the chaotic signal x(t),which is sampled to generate the impulsive series x(k$\mathbf{\Delta T}$) with rate $\mathbf{1/\Delta T}$. The series data is first stored in a buffer and then delivered to the driven system with rate $s/\Delta T$. The state variables of the driven system are subject to jumps at discrete instants, $t = i\Delta T/s$ $i = 0,1,2 \ldots$. The driven system is governed by

$$y = sAy + s\dot{F}(y) \qquad t \neq i\Delta T/s \tag{15}$$

$$\Delta y|_{t=\frac{i\Delta T}{s}} = y(t^+) - y(t^-) = \boldsymbol{B}e \qquad i = 0,1,2 \ldots \tag{16}$$

where **B** is a constant matrix and

$$e(t) = x(st) - y(t) \tag{17}$$

is the synchronization error. The mechanism behind this proposed scheme is the impulsive synchronization theory. Under suitable choice of **B** and ΔT the system in Equation (15) will synchronize with the system in Equation (12).

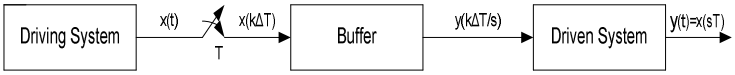

Figure 5: Block diagram for generating time scaling chaotic signal

Figure 6 shows the implementation of the ambiguity diagram. The driving system generates a chaotic signal, which is sampled at the interval ΔT. The sampled signal x(kΔT) is going through two channels the upper channel is used to generate the time scaling version of the chaotic signal x(t) as discussed in the last section. The lower channel is used to generate the time-delay version of the chaotic signal x(t). The two channel outputs are used to perform the correlation operation. The correlation output is the desired AF value at specified (s,τ). By changing(s,τ)we can get the whole AF diagrams of the chaotic signals.

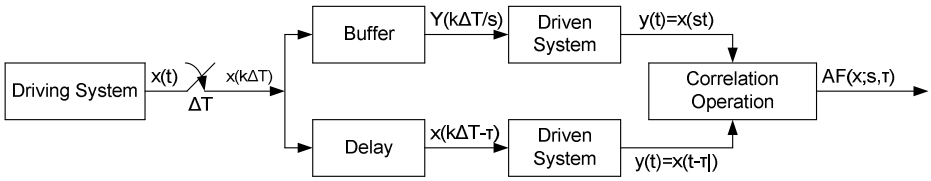

Figure 6: Schematic block diagram for AF calculation

Brown (1992; 1993) developed a general method of expressing any dynamical system into a general form called type II generalized Chua equation. To apply the impulsive synchronization theory to determine the Rossler system of equations ambiguity diagram, it needs to be expressed in this generalized form. Let the solutions of the following vector ordinary differential equation be unique in a bounded region R^n(n dimensional vector)

$$\dot{x} = \boldsymbol{A}(x)\big(x - \boldsymbol{F}(x)\big) \tag{18}$$

where A(x) is an n×n matrix function of x and F is a function mapping R^n to itself. A type II generalized Chua equation is an ordinary differential equation of the above form in which the components of the matrix $\boldsymbol{A}$ and the vector function $\boldsymbol{F}$ are composed of finite linear combinations of sigmoid functions. In addition to the usefulness of this equation for analysis, there are numerical advantages for modeling and simulation in that we are able to generate simple maps that are easy to evaluate on a computer and which have a wider range of dynamics. The choice of Rossler parameters found to give the optimal ambiguity function are $a = 0.398, b = 0.2, c = 4$ and when substituted in the Rossler dynamics gives

$$\begin{pmatrix}\dot{x}(t)\\ \dot{y}(t)\\ \dot{z}(t)\end{pmatrix} = \begin{bmatrix}0.0 & -1.0 & -1.0\\ 1.0 & 0.398 & 0.0\\ 0.0 & 0.0 & -4.0\end{bmatrix}\begin{pmatrix}x\\ y\\ z\end{pmatrix} + \begin{pmatrix}0.0\\ 0.0\\ 2.0 + xz\end{pmatrix} \tag{19}$$

The fixed points for the Rossler system of equations are determined to be:

$$x_0 = 2 \pm 1.7899\ ,\ y_0 = -x_0/0.398\ \ ,z_0 = -y_0 \tag{20}$$

For reasons of convenience (Carrol, T. L. and Pecora L. M., 1991) we write x_0 as

$$x_0 = 2 \pm \lambda \tag{21}$$

where $\lambda = 1.7899$.

Using the λ the linear part of the vector field at these fixed points is given by

$$A = \begin{bmatrix}0.0 & -1.0 & -1.0\\ 1.0 & 0.398 & 0.0\\ (2 \pm \lambda)/0.398 & 0.0 & -2.0 \pm \lambda\end{bmatrix} \tag{22}$$

The function F(x) serves to define the fixed points of the type –II generalized Chua equation. It is determined by the fixed points of the Rossler equations. Hence from equations (20) and (21) F(x) is given by

$$F(x) = \begin{bmatrix}2.0 \pm \lambda\\ -(2 \pm \lambda)/0.398\\ (2 \pm \lambda)/0.398\end{bmatrix} \tag{23}$$

Equations (22) and (23) are substituted in the driving and the driven systems as given by equations (12) and (13). This gives the desired type-II Chua equation for implementation. For chaotic systems $y(t) \to x(st)$ as $t \to \infty$ when ΔT satisfies (Brown R., 1992; 1993)

$$\Delta T = \frac{\ln(\xi d_1)}{q+2|\alpha a|}, \xi \to 1 \qquad (24)$$

where d_1 is the largest eigenvalue of $(I + B^T)(I + B)$ and q is the largest of $(A + A^T)$ a is a constant and I is an identity matrix. The proof can be found in (Tao, Y. and Chuo, L. O., 1997). In the following MATLAB Simulations the function "ode45" is used to solve (23) and (24) with step size 10^{-5} $a = 1$ and initial conditions set as $\big((x_1(0), x_2(0), x_3(0)) = (-0.4, -0.6, 0.7)\big)$ and $((y_1(0), y_2(0), y_3(0))$ = (1, 0, 0). The matrix **B** is chosen as (Brown, R., 1993)

$$\boldsymbol{B} = \begin{pmatrix} -1.1 & 0 & 0 \\ 0 & -1 & 0 \\ 0 & 0 & -1 \end{pmatrix}$$

The other parameters are chosen as $(a, b, c, s) = (0.398, 2, 4, 1)$.
By implementing each of the functions in Figure 6 using MATLAB Simulink toolbox and the user defined System-function provision in the Simulink the ambiguity diagram in the contour form was obtained as shown in Figure 8.

4. Simulation Results and Discussion

4.1 The Ambiguity diagram

Figure 7 and 8 shows the ambiguity diagrams of the LFM waveform and the Rossler waveform respectively. While that of the LFM is smooth having its peak at A1 and no side lobes that of the Rossler waveform peaks at A with some minor lobes labelled D. The minor lobes indicate possible presence of clutter, or the undesired echo from the radar environment as a result of using this waveform but these can be easily eliminated through filtering.

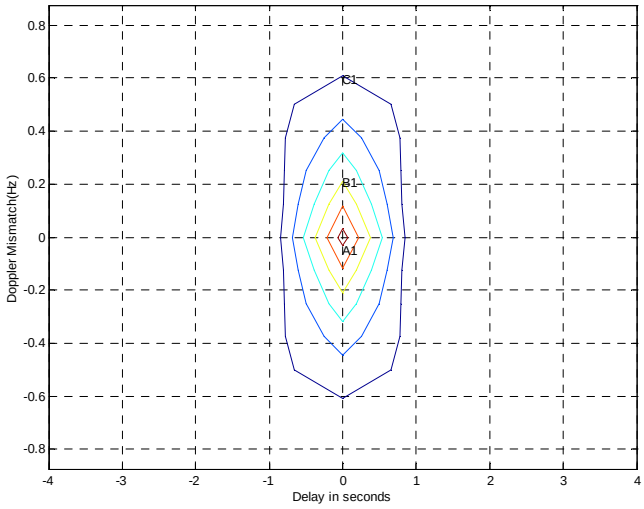

Figure 7: Ambiguity diagram of an LFM Waveform

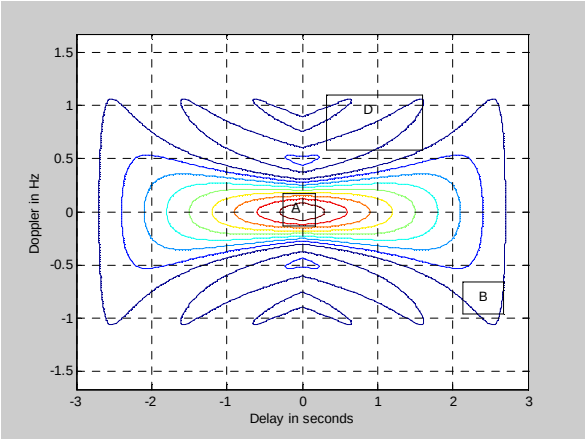

Figure 8 : Ambiguity diagram of the Rossler Waveform

4.2 The bandwidth of the Waveform

The LFM waveform has an instantaneous frequency that linearly increases or decreases with time. The set of LFM waveforms thus includes only two quasi –orthogonal waveforms, that is 'up-chirp' when the frequency is increasing linearly and 'down-chirp' when the frequency is decreasing linearly. Figure 9 shows the up-chirp LFM waveform and its fast Fourier transform. As is the case with discrete Fourier transforms the first $\frac{N}{2}$ samples contains the positive frequency components and the negative frequency components appear in the second half of the array. Only one half of the spectrum needs to be transmitted.

From the result of Figure 10 it is clear that if the control parameters a, b and c are kept constant and the scaling factor q is varied then the bandwidth of the waveform varies within some limit. This implies that a random choice of q , will result in different independent waveforms with different spectral components. However for large variations the control parameters must be varied. This important since the control parameters determines whether the system operates in the chaotic region or not.

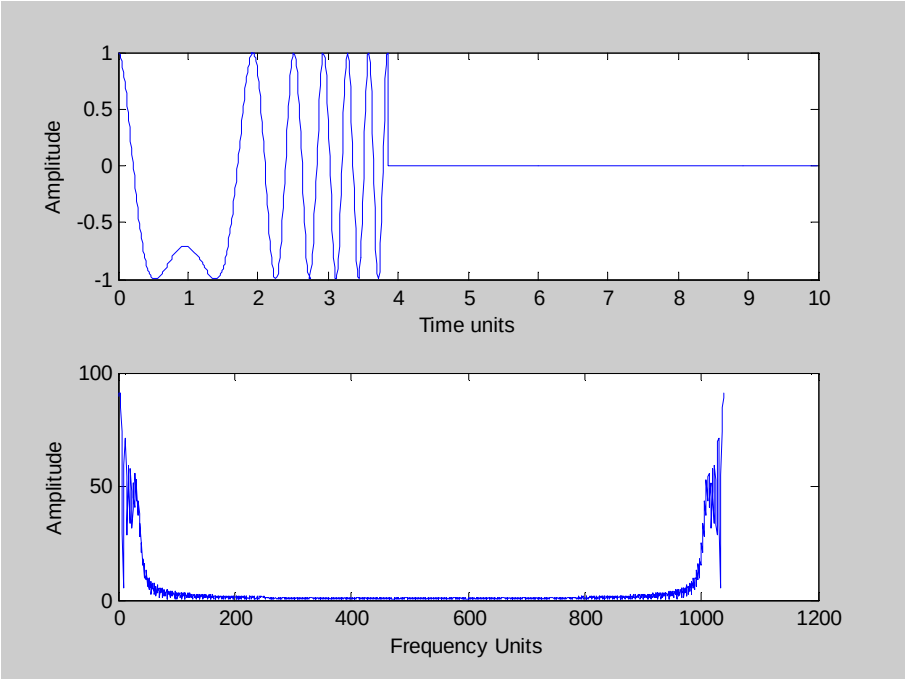

Figure 9: Up chirp LFM Waveform and its Frequency Spectrum

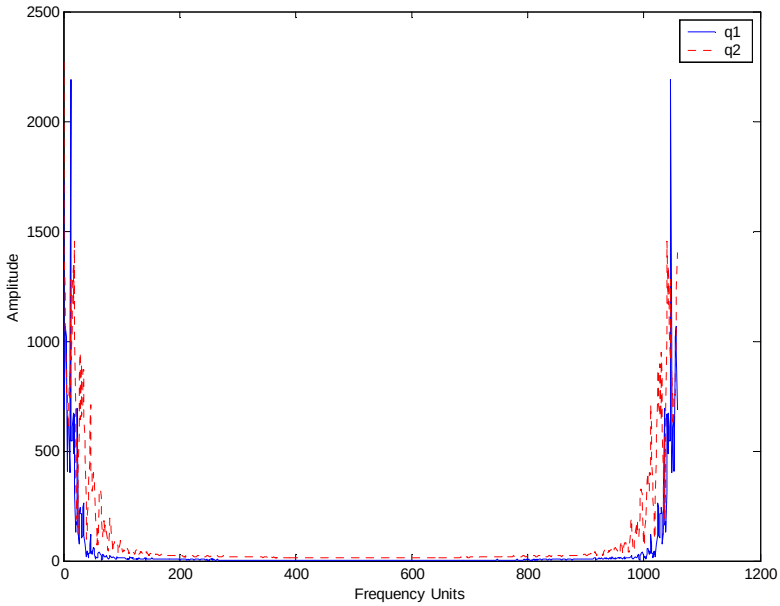

Figure 10: Variation of the bandwidth of the Rossler waveform with the scaling factor

From Figure 10,for the control parameter $q1 = 1$,the spectral component of the Rossler waveform is almost identical to that of the LFM in Figure 9. However, an increase of the scaling parameter to $q2 = 2$, reduces the bandwidth as predicted by Equation (11). The importance of this is that by varying q, different Rossler waveforms with different spectral components will be obtained.

5. Conclusion

This paper proposed the use of Rossler waveform to generate and optimize independent waveforms that can be used in MIMO radars. It has been observed that by variation of the parameters different waveforms of different frequency components can be generated, unlike the LFM where only to independent waveforms is possible. By using the ambiguity diagram it is shown that these waveforms meet the requirements of radar waveforms and compares well with the LFM waveforms. The ambiguity diagram can be adjusted to obtain a sharp peak, a key requirement in fine and Doppler and range resolution. By using a scaling factor the bandwidth of the Rossler waveforms can easily be scaled to the desired range. With the inherent characteristics of chaotic waveforms that includes possibility of secure detection and low probability of intercept because of their quasi random nature, the Rossler waveforms would be ideal for use as radar waveforms. However these two metrics cannot be considered in isolation and this research now focuses on the other metrics for evaluating the radar waveform metrics such as the autocorrelation and cross correlation functions. The other metrics to be considered is the Peak-to-RMS ratio which determines the amount of power that can be transmitted.

References

Brown, R. (1993) Generalization of Chua circuits" *IEEE transaction on circuits and systems-Fundamental theory and Applications*. **40** (11) pp. 523-526.

Brown, R. (1992) Generalizing the Chua Equations, *Int. Journal of Bifurcation and Chaos*, **2**, (4) pp. 703-707

Carrol, T. L., and Pecora, L. M. (1991) Synchronization chaotic circuits. *IEEE Transactions on circuits and Systems*, **38**, pp. 453-456.

Cheng, Hu *et al* (2010) Impulsive control and Synchronization for delayed neural networks with Reaction-diffusion terms" *Circuits and Systems*, **2**(1) pp. 611-614.

Das, A. and Lewis, F. L. (2010) Distributed adaptive control for synchronization of unknown non linear networked systems. *Automata* **46**(12) pp. 710-714.

Hu, H. P. and Zhu, Z. (2010) Robust Synchronization by Time-Varying Impulse .*Control, Circuits and Systems, IEEE Transactions* 58,(12) pp. 2882-2893.

Levanon, N. and Mozeson, E. (2004) *Radar Signals*. New York: Wiley-IEEE Press.

Lewis, F. L. and Das, A. (2011) Distributed adaptive control for synchronization of unknown non linear networked systems. *Automatica*, **46**(12), pp. 2014-2021.

Lin, F. Y. and Liu, J. M. (2004) Quantum Electronics. *IEEE Journal* **40**, pp. 815.

Lu, J.G. (2010) Impulsive Synchronization of chaotic Lur'e Systems by Linear Static Measurement Feedback: An LMI approach. *Circuits and Systems* **54**(8) pp. 710-714.

Lu, W. L. (2007) Adaptive dynamical networks via neighborhood Information: Synchronization and pinning control. *Chaos*, **17**(2) pp. 2231-2232.

Pecora, L. M. and Carrol, T. L. (1988) Master Stability functions for synchronized coupled systems. *Phy. Rev. Lett.*, **80** (2) pp. 2109-2112.

Ramirez, A. B. and Rivera, I. J. (2005) SAR image processing algorithms based on the ambiguity function .*Circuits and Systems* , *IEEE transactions*,**2** pp. 1430-1433.

Rossler, O. E. (1976a) An equation for continuous chaos. *Phys. Lett.***57** pp. 397-398.

Skolnic, M. I. (2001) *Introduction to Radar Systems*. New York: McGraw-Hill.

Tao, Y. and Chuo, L. O. (1997) Impulsive stabilization for control and synchronization of chaotic signals: Theory and applications to secure communication. *IEEE transactions on circuits and systems*,**44** pp. 976-988.

Willsey, M. (2006) Quasi *Orthogonal Wideband Radar Waveform Based On Chaotic Systems*. Unpublished thesis (Msc.), Massachusetts Institute of Technology.

Woodward, P. M. (1967) Radar Ambiguity Analysis. *Royal Radar Establishment* **30**, pp. 731.